

## Effect of the intermediate principal stress on strength and deformation behavior of sedimentary rocks at the depth shallower than 2000 m

Effets de la contrainte principale intermédiaire sur la résistance et la déformabilité des roches sédimentaires à une profondeur inférieure à 2 000 m

Einfluß der mittleren Hauptspannung auf das Festigkeits- und Verformungsverhalten von Sedimentgesteinen bis 2000 m Überlagerung

M.Takahashi & H.Koide  
*Geological Survey of Japan, Japan*

**ABSTRACT:** To clarify the effect of the intermediate principal stress on the strength and deformational behavior of rocks, three sandstones, marble, and shale were deformed under true triaxial stress state in which the intermediate principal stress is not equal to the minimum nor to the maximum principal stress. Failure strength increased with the relative increase of the intermediate principal stress except for the stress state where the intermediate principal stress approaches to the maximum stress. The relative increase of intermediate principal stress induced also changes the deformation of rock from the ductile mode to the more brittle mode. The difference between the intermediate principal strain and minimum principal strain increased markedly with increment of the intermediate principal stress. The fracture stability of rock specimen was suggested by the concept of the effective shear strain energy stored around the closed microcracks. The deformational anisotropy was indicated by the preferred orientation of stress-induced open microcracks.

### 1 INTRODUCTION

The physical behavior of rock under triaxial stress state is essentially important for the underground mining and for the utilization of underground spaces (for example, tunnels, electric powerhouse, storages of gas and oil, open pit mine, and high level waste repository and so on), because the act of excavations changes the stress fields and other physical and mechanical environments of rocks around the underground open space.

The underground rock body is subjected to the initial stress prior to excavation. In many cases, it can be adequately assumed that the vertical normal stress is equal to the weight of the overlying rockmass, usually, 25-27MPa/Km on the average. The magnitude of the horizontal stresses lie widely between 0.5 and 3.5 times as large as the vertical normal stress at the depth shallower than 1000m (Brown and Hoek, 1978). These observations suggest that the three principal stresses are different each others for many cases of initial and artificial stress state. In order to investigate the mechanical characteristics of rocks around the underground openings, we have to adopt the testing equipment with which three different principal stresses can be reproduced precisely.

The so-called triaxial compression test has been proved to be the most adequate and convenient testing method for the study of the mechanical characteristics of rocks for wide variety of confining pressures. In the conventional triaxial compression test, the longitudinal axial load is applied parallel to the axis of a cylindrical rock specimen through steel end pieces and the other stresses (confining pressure) are the cylinder by a fluid medium. The relatively homogeneous stress distribution can be produced in the specimen with the conventional triaxial test (confining pressure test). However, the intermediate principal stress is fixed equal to the minimum principal stress (compression test under confining pressure), in fewer cases, to the maximum principal stress (extension test under confining pressure), because the stress state in the confining pressure test is essentially axially symmetrical. According to the confining pressure experiments, failure strength increased remarkably with increase of the confining pressure, and relative transition from brittle to ductile behaviors is observed by the increase of the confining pressure. Thus, conventional triaxial experiment has been executed to elucidate the confining pressure effect on strength and deformation of rocks. However, these confining

pressure experiment is not adequate for decision of mechanical properties of rocks around the underground open spaces. Because these confining pressure experiment can reproduce only the axially symmetrical stress states.

On the other hand, a fundamental problem of rock mechanics remained unsolved. Whether the intermediate principal stresses affect on the failure strength and deformation of rocks or not? The effect of the intermediate principal stress had been studied by some investigators using various experimental techniques. Mogi(1967) carried out precise experiments of the compression and extension tests under confining pressure, and found clear differences between the Mohr envelopes of stress states with the intermediate principal stress equal to the maximum stress and equal to the minimum stress for three kinds of rocks. He verified the existence of the intermediate principal stress effect on failure strength. Hojem and Cook(1968) constructed a polyaxial cell for the test of rectangular specimens of rock (1"x1"x 3"). Lateral sides of the specimen are confined between two pairs of copper flat-jacks. They detected a small amount of failure strength increase with increasing intermediate principal stress for Karroo dolerite at minimum principal stresses of 1 kpsi and 2 kpsi. Akai and Mori(1967), Niwa et al.(1967), and Serata et al.(1972) carried out triaxial compression tests, where three pairs of mutually perpendicular pistons applied three principal stresses to cubic specimen through steel end pieces which are more rigid than the rock specimen. They also found the intermediate principal stress effect for Izumi sandstone, salt, concrete mortar and so on. Mogi(1971) designed a new triaxial cell which is a thick-walled hollow cylinder with two pairs of mutually perpendicular diametrical holes for axial and lateral pistons. Thus, the new triaxial cell makes possible to do the biaxial deformation test in the pressured fluid. Usually, the minimum principal stress is induced by the fluid pressure, while the maximum and intermediate principal stresses are applied with the two pairs of rigid pistons. Eventually, three principal stresses can be controlled independently in this vessel. The stress distribution in the specimen of this new true triaxial test is more homogeneous than in the specimen which is compressed with rigid pistons on its all six sides. Using this new true triaxial apparatus, Mogi solved the problems of the low reproducibility and of low accuracy of triaxial experiments. Mogi(1971a,b,

1972a,b, 1973, 1977) clarified that strength and ductility of isotropic rocks are markedly affected not only by the least principal stress, but also by the intermediate principal stress, and that dilatancy is highly anisotropic under the relatively higher intermediate principal stress states.

In this study, a large Mogi-type triaxial cell was designed to allow the use of large specimen and relatively easy measurement of physical properties. The failure strength, the stress drop at fracture, and three principal strains were systematically measured for some kinds of sandstone and shale under the true triaxial stress state with the Mogi-type new apparatus. The minimum stress in this experiments is much lower than in the Mogi's experiments, because such low compression states are more important for engineering applications.

## 2 EXPERIMENTAL APPROACH

Fig-1 shows a schematic view of new Mogi

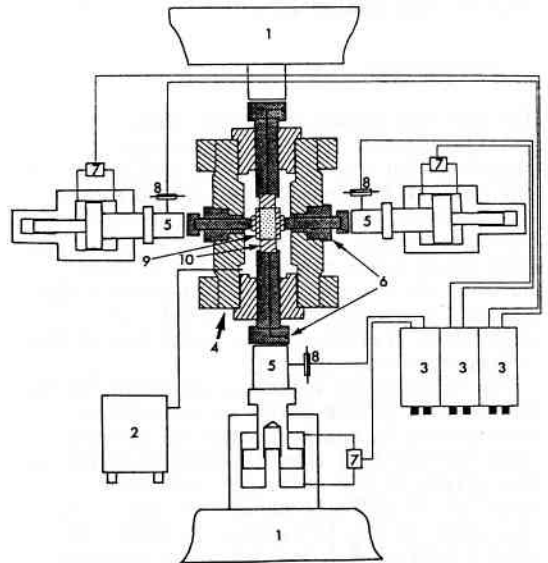


Fig.1 Schematic diagram of a new designed true triaxial compression apparatus. 1:Fixed Upper and Lower Platen, 2:Hydraulic Power Supply, 3:Control Unit, 4:Pressure Vessel, 5:Load Cells for Axial and Lateral Direction, 6:Pistons for Axial and Lateral Load, 7:Servo Valve, 8:Displacement Transducers for Axial and Lateral Deformation, 9,10:Lateral and Axial End Pieces.

type triaxial apparatus developed for this true triaxial compression test. Maximum and intermediate principal stresses are applied through two pairs of rigid pistons, and minimum principal stress is applied by confining pressure medium in the vessel. The specimen was a rectangular prism of 3.5x3.5x7.0 cm long ( maximum size was 5.0x5.0x10.0cm long ). The end pieces for maximum compression are connected to a specimen with epoxy and lateral end pieces are connected to the sides of the specimen through a lubricant(thin copper sheet and teflon sheet with silicon grease), by which the frictional effect of lateral surfaces was effectively reduced. As this apparatus adopted the electric-hydraulic servo-controlled system, the specimen can be deformed at arbitrary constant stress state. New triaxial cell is set up with pressure-tight windows for electrical feeders for measurements of strain, acoustic emission, elastic wave velocity and so on. We can measure the strain with 56 pairs of strain gauges attached directly on the specimen in the pressure vessel.

Fig-2 shows three different types of loading path. For the conventional confining pressure experiment(a), the confining pressure was first applied, and then the larger compression is applied through steel end pieces which are more rigid than the rock. In the typical case of triaxial compression experiment(b), the confining pressure was first applied, and the lateral load for  $\sigma_2$  was increased to a constant value of  $\sigma_2$  by lateral piston, then, the axial load was increased by axial piston with constant rate until failure occurred. In our experiment, this (b) type loading path was used frequently. The loading procedure (A-B) in (b) type correspond to that procedure (A-C) in type (a), there is possibility that specimen may fail when load increment on (A-B) path is so large. To avoid such risk, (c) type loading path was adopted for some triaxial compression test with high intermediate stress. The confining pressure first applied as well as previous (a), (b) cases, and lateral and axial loads were applied simultaneously to a constant  $\sigma_2$  value. The axial load, then, was increased higher to deform the specimen, this (c) type loading path, as it is rather complicated to test, used rarely.

Directions of the X-axis, Y-axis, and Z-axis are taken as the directions of  $\sigma_1$ ,  $\sigma_2$ , and  $\sigma_3$ , respectively. The compressive stress is taken as positive.  $\epsilon_x$ ,  $\epsilon_y$ , and  $\epsilon_z$  are the principal strains for the directions of X-, Y-, and Z-axis, respectively. The axial strain  $\epsilon_z$  and

lateral strain  $\epsilon_y$  were measured by cross-type electric resistance strain gages mounted on the surfaces of specimen perpendicular to the X-axis (Fig-3). The lateral strain  $\epsilon_x$  for  $\sigma_3$  direction was measured by the displacement transducers, which can detect the changes of the width of the specimen in the X direction using strain gages mounted on the phosphor bronze sheet, of which one end was fixed to the specimen surfaces and the other was fixed to the upper end pieces in the axial direction. Three principal strains are defined as the strains due to the increase of the axial stress under the constant  $\sigma_2$  and  $\sigma_3$ . Thus, in Fig-2(b) strains for

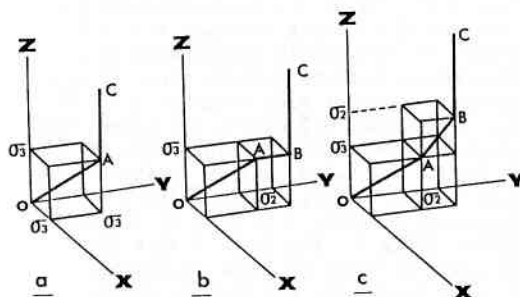


Fig.2 Three different loading paths in a triaxial compression. Points A,B,C illustrate a Hydraulic pressure, intermediate principal stress, and fracture strength respectively.

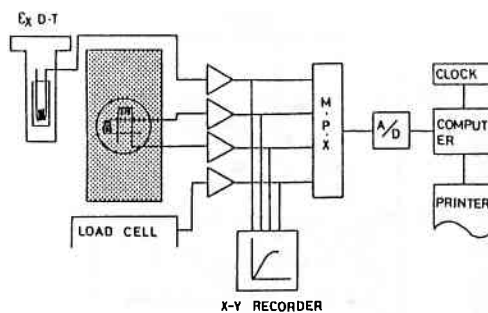


Fig.3 Schematic view of strain measuring system

three principal directions were measured as the interval between point B and point C.

In present paper, the Shirahama medium grained sandstone, Horonai fine and medium grained sandstones, Yuubari shale were used for specimen. Two Horonai sandstones and Yuubari shale were cored from the block which were sampled in Horonai and Yuubari coal mine at central Hokkaido, Japan.

### 3 EXPERIMENTAL RESULTS

The intermediate stress effect on strength is clearly shown on the maximum stress ( $\sigma_1$ ) vs intermediate stress ( $\sigma_2$ ) diagram (Fig.4 to Fig.8). The fracture strength of Shirahama sandstone is indicated in the Fig.4 as a function of intermediate principal stress ( $\sigma_2$ ) for various minimum stress ( $\sigma_3$ ). In this figure, each symbols at the most left side show results obtained under confining pressure experiment, that is,  $\sigma_2 = \sigma_3$ . Therefore, the fracture strength of rocks at constant  $\sigma_3$  value can locate between this confining compression stress state ( $\sigma_2 = \sigma_3$ ) and confining extension stress state ( $\sigma_1 = \sigma_2$ ). Since  $\sigma_1$  increased with the increase of  $\sigma_2$  under constant  $\sigma_3$ ,  $\sigma_2$  effect on strength is represented as a discrepancy between maximum strength and minimum one under wide range of  $\sigma_2$ . At low  $\sigma_2$  region,  $\sigma_2$  effect was large, and gradually decreases with increment of  $\sigma_2$ . At higher  $\sigma_2$  value,  $\sigma_1$  is constant (in case of  $\sigma_3 = 15\text{MPa}$ ,  $40\text{MPa}$ ,  $50\text{MPa}$ ) or decreases slightly (in case of  $\sigma_3 = 8\text{MPa}$ ,  $20\text{MPa}$ ,  $30\text{MPa}$ ). Fig-5, 6, 7 show the fracture strength of Izumi sandstone, Horonai sandstone, and Yuubari shale, respectively. The  $\sigma_2$  effect on strength of each rocks becomes more distinct at higher minimum stress. The Yamaguchi marble shows very large effect of the intermediate

principal stress (Fig.8). This distinctive difference between Yamaguchi marble and the other rocks on the  $\sigma_2$  effect, discussed latter, was caused by the difference of the deformational characteristic.

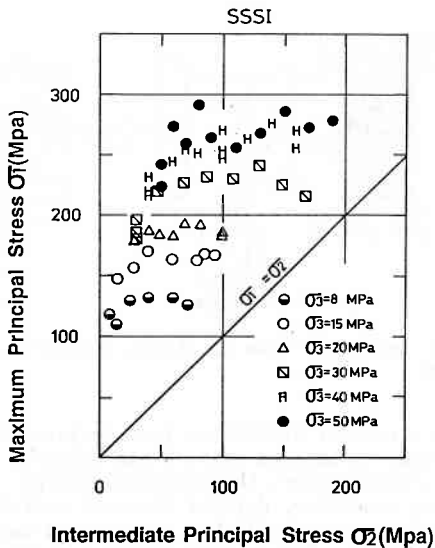


Fig.4 Fracture strength ( $\sigma_1$ ) as a function of the intermediate principal stress ( $\sigma_2$ ) in Shirahama sandstone.

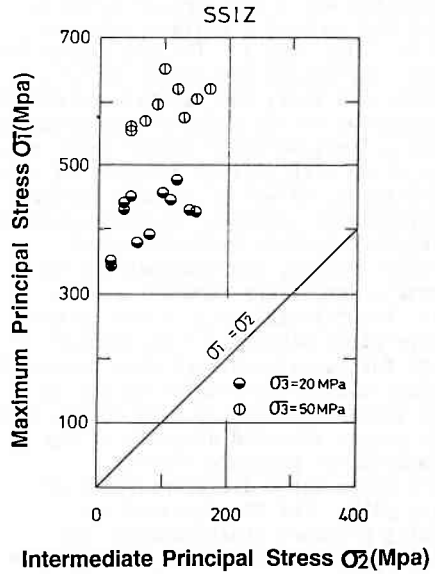


Fig.5 Fracture strength as a function of the intermediate principal stress in Izumi sandstone.

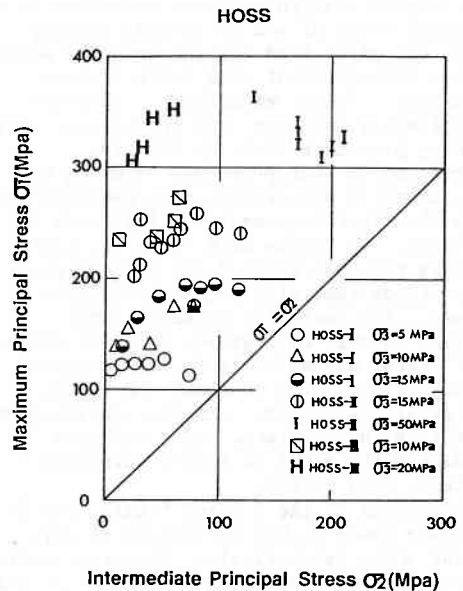


Fig.6 Fracture strength as a function of the intermediate principal stress in Horonai sandstone.

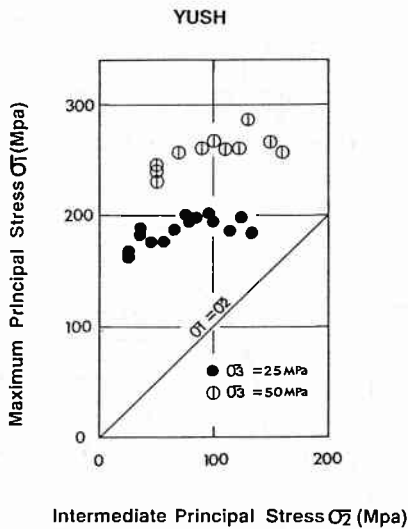


Fig.7 Fracture strength as a function of the intermediate principal stress in Yuubari shale.

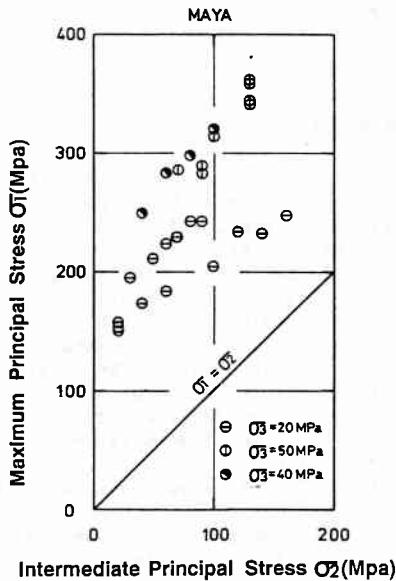


Fig.8 Fracture strength as a function of the intermediate principal stress in Yamaguchi marble.

If the stress state of rock specimen reaches the maximum strength, rock specimen will fail and the sudden stress drop of axial stress accompanying fracture occurs. The residual strength is defined as the strength of specimen which already

experience major failure. In the Shirahama sandstone and Yuubari shale, typical macroscopical fault plane is formed parallel to the  $\sigma_2$  direction. Thus, residual strength means the shear resistance of fault planes. Although the residual strength scattered within some value, it is recognized that residual strength remains nearly constant in spite of the change of the intermediate principal stress (Fig.9).

Fig-10 shows stress-strain curves as a function of axial differential stress for the four different  $\sigma_2$  values. Specimen was the Shirahama sandstone and confining pressure was kept constant of 50MPa. The upper left figure shows the case of the axi-symmetric stress state ( $\sigma_2 = \sigma_3 = 50$ MPa). In this case,  $\epsilon_x$  and  $\epsilon_y$  (lateral principal strain for  $\sigma_2$  and for  $\sigma_3$  direction) are nearly equal. The lower right figure shows a typical case of true triaxial stress state ( $\sigma_2 = 190$ MPa). In this case, the maximum strength is higher than that in the case of the axi-symmetric stress state, lateral strain  $\epsilon_x$  for the  $\sigma_3$  direction is much greater than that for the  $\sigma_2$  direction. It is obviously noted that  $\epsilon_x$  differed more distinctly from  $\epsilon_y$  with increase of  $\sigma_2$ . In the Fig-11, the four different volumetric strain versus differential stress curves were extracted from the Fig-10. The dotted line corresponds to the elastic volumetric strain. The dilatant strain indicated by hatched region decreases with increment of  $\sigma_2$  value. We can consider that the

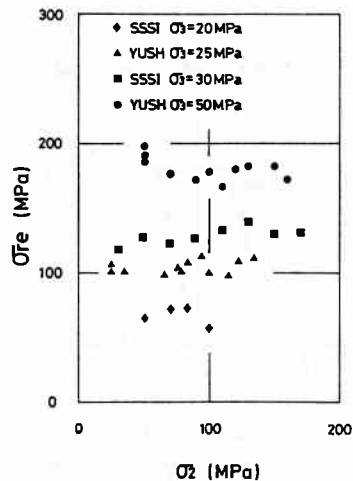


Fig.9 Residual strength ( $\sigma_{re}$ ) as a function of the intermediate principal stress in Shirahama sandstone.

dilatant strain is mainly caused by the increment of lateral strain in the  $\sigma_3$  direction at higher  $\sigma_2$  value.

Fig.12 shows a series of axial differential stress versus strain curves of Yamaguchi marble for different  $\sigma_2$  values under constant minimum stress of 20MPa. In this experiment, although the strain at ultimate strength decreased slightly with increase of  $\sigma_2$ , ultimate strength increased with the increase of  $\sigma_2$ . Under

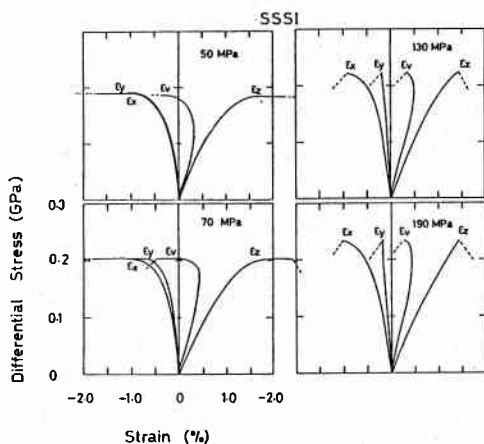


Fig.10 Differential stress - axial, lateral, and volumetric strain curves of Shirahama sandstone under the four different intermediate principal stresses. Minimum stress is fixed to 50MPa.

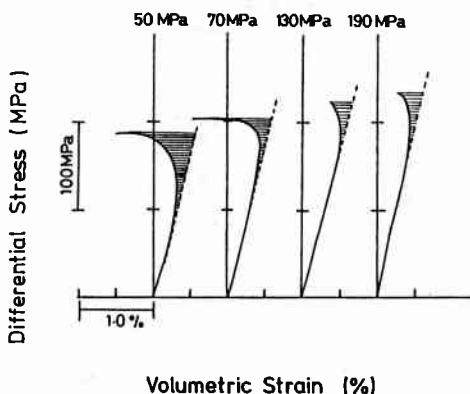


Fig.11 Differential stress versus volumetric strain of Shirahama sandstone under the four different intermediate stresses. Hatched region indicate the dilatant strain.

axially-symmetric stress state, this marble behaved as ductile. However, the more stress drop at failure occurred at relatively higher intermediate principal stress. The marble behaved in brittle mode at the highest  $\sigma_2$  value in the Fig.12.

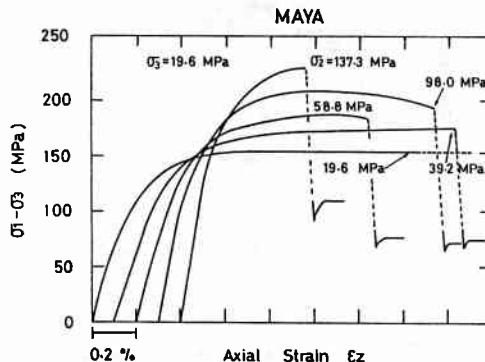


Fig.12 Differential stress versus axial strain of Yamaguchi marble for the five different  $\sigma_2$  under constant confining pressure of 20MPa.

#### 4 DISCUSSION

The accepted criteria for the strength of rock, such as Coulomb, Mohr, and Griffith criterion, are essentially independent of the intermediate principal stress. However, the experimental observations suggest apparently that the intermediate principal stress has a dominant and regular effect on strength of rocks. When we discuss on rock strength, we must consider the existence of  $\sigma_2$  effect on rock strength. In this paper, a criterion developed by Wiebols and Cook(1968) for the compressive strength of rock is modified.

The following three assumptions are made.

- (1) rock specimen can be regarded as an elastic materials containing a large number of closed microcracks
- (2) any closed microcracks distributed randomly oriented and did not correlate with each other
- (3) this rock specimen can be regarded as a grossly homogeneous

The surfaces of any closed microcracks can be subject to normal stress " $\sigma_n$ " and shear stress " $\tau$ " under compressive stress state. The normal stress and shear stress on any closed microcracks are defined

- (1)  $\sigma_n = l^2 \sigma_1 + m^2 \sigma_2 + n^2 \sigma_3$
- (2)  $\tau^2 = l^2 \sigma_1^2 + m^2 \sigma_2^2 + n^2 \sigma_3^2$
- (3)  $\tau_{eff} = |\tau| - \mu \sigma_n$

where  $\tau_{eff}$  is the effective shear stress,  $\mu$  is the coefficient of friction between the opposite surfaces of the closed microcracks, and  $l, m, n$  are the direction cosines of the normal of the crack surface to the principal stress axes. If  $\tau_{eff}$  is positive, sliding occurs between the opposite surfaces of the closed microcracks, storing additional strain energy around the closed microcrack. The additional strain energy around a crack due to sliding is given

$$(4) \quad W_c = a \tau_{eff}^2$$

where  $a$  is constant containing some factors of the closed microcrack and matrix. The total additional strain energy can be summing  $W_c$  for each crack through a unit volume of rock subject to stress. In original theory, Wiebols and Cook(1968) assumed that fracture occurs when shear strain energy stored in rock is equivalent to that of uniaxial compression. However, their analyses could not predict the strength of various kinds of rock. The predicted intermediate stress effect is larger than that in the experimental results. Thus, we propose that maximum shear strain energy stored in rock specimen should be function of  $\sigma_2$  and  $\sigma_3$  values. According to our experimental results, failure criterion using the concept of effective shear strain energy, could be expressed using the concept of effective shear strain energy as follows.

$$W_{err}(\sigma_2 = \sigma_3) = W_{err}(C_0) \left\{ 1 + C \frac{\sigma_3}{C_0} \right\} \\ \sigma_2 = \sigma_3 < \sigma'_3$$

$$W_{err}(\sigma_2 = \sigma_3) = W_{err}(C_0) \times a \\ \sigma_2 = \sigma_3 > \sigma'_3$$

$$W_{err} = W_{err}(\sigma_2 = \sigma_3) \left\{ 1 - b \frac{\sigma_2}{\sigma_3} \right\} \\ \sigma_2 > \sigma_3$$

where  $a, b, c$  are constants, which depend on rock specimen itself,  $\sigma'_3$  and  $C_0$  is a specific confining pressure and uniaxial compressive strength of each rock.  $W_{eff}(C_0)$ ,  $W_{eff}(\sigma_2 = \sigma_3)$ , and  $W_{eff}$  mean the maximum shear strain energy under uniaxial compression, under axi-symmetric stress state, and under true triaxial compression

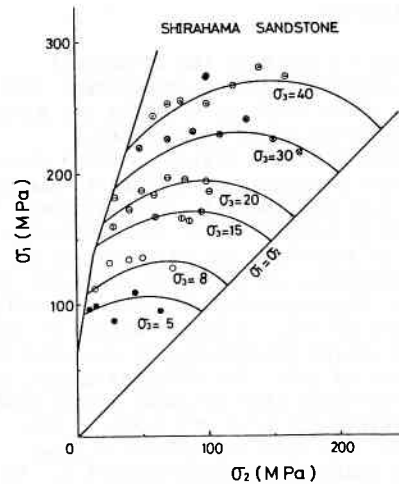


Fig.13 Prediction of the fracture strength of Shirahama sandstone based on the modified effective shear strain energy criterion. Prediction is shown by the solid curves.

stress state, respectively. The observations for various  $\sigma_3$  values on Shirahama sandstone are illustrated in Fig-13, and they are reasonably consistent with the modified effective shear strain energy criterion.

The strong anisotropy of dilatancy to the  $\sigma_2$  direction and to the  $\sigma_3$  direction indicates that the stress-induced microcracks are created preferentially perpendicularly to the  $\sigma_3$  direction in a rock during axial loading under true triaxial stress state.

The normal stress to the wall of a unlined underground cavern is equal or nearly equal to the atmospheric pressure in the host rocks close to the wall of cavern. The microcracks should be formed nearly parallel to the wall of cavern, as the minimum stress is perpendicular to the wall. The results of true triaxial tests suggest that the brittle failure of rock is likely under the very low minimum stress with relatively high intermediate principal stress in the wall rock of unlined underground cavern. The increase of the normal stress to the wall of cavern by the artificial supports can prevent the sudden brittle failure as well as the drastic increase of effective strength of the wall rock. The estimation of true triaxial stress condition in the wall rock is essentially important for the maintenance of the underground cavern.

## 5 CONCLUSION

In order to estimate the mechanical characteristics around underground open space, three sandstones, shale and marble were deformed under true triaxial compression stress state, in which three principal stresses are different from each other and independently controllable. The minimum principal stress was adopted up to 50MPa to reproduce the stress state around the excavation at the depth shallower than 2000m. Fracture strength increased with increase of  $\sigma_2$ . Dilatant strain to the  $\sigma_2$  direction decreased with the relative increase of  $\sigma_2$ . The dilatant anisotropy occurred under true triaxial stress state with relatively high  $\sigma_2$  value in the result. The modified effective shear strain energy criterion proposed in this paper can explain well the observations on strength characteristics. The true triaxial test of rock is very important for the estimation of stability of wall rock of underground caverns.

## REFERENCES

- Akai, k. and Mori, H. 1967. Study on the failure mechanism of a sandstone under combined compressive stresses (in Japanese). Proceedings of J.S.C.E 147: 11-24.
- Brown, E.T. and Hoek, E. 1978. Trends in Relationships between measured in-situ stresses and depth. Int.J.Rock.Mech. Min.Sci.Geomech.Abstr 15: 211-215.
- Mogi, K. 1967. Effect of the intermediate principal stress on rock failure. J.Geophys.Res 72: 5117-5131.
- Mogi, K. 1971a. Effect of the triaxial stress system on the failure of dolomite and limestone. Tectonophysics 11: 111-127.
- Mogi, K. 1971b. Fracture and flow of rocks under high triaxial compression. J.Geophys.Res 76: 1255-1289.
- Mogi, K. 1972a. Fracture and flow of rocks. Tectonophysics 13: 541-568.
- Mogi, K. 1972b. Effect of the true triaxial stress system on fracture and flow of rocks. Phus.Earth Planet.Inter 5: 318-324.
- Mogi, K. 1973. Rock fracture. Annual Review Earth Planet.Sci 1: 63-84.
- Mogi, K. 1977. Dilatancy of rocks under general triaxial stress states with special reference to earthquake precursors. J.Phys.Earth 25:s203-s217.
- Niwa, Y. et al. 1967. Failure criterion of leightweht concrete to triaxial compression (in Japanese). Proc.J.S.C.E 143:28-35.
- Serata, S. 1968. Application of continuum mechanics to design of deep potash mines in Canada. Int.J.Rock.Mech.Min.Sci 5: 293-314.
- Wiebols, G.A. and Cook, N.G.W. An energy criterion for the strength of rock in polyaxial compression. Int.J.Rock.Mech.Min.Sci 5: 529-549.

PROCEEDINGS / COMPTES RENDUS / BERICHTE  
ISRM-SPE / INTERNATIONAL SYMPOSIUM / PAU / 1989.08.28-31

# Rock at Great Depth

*Rock mechanics and rock physics at great depth*

*Mécanique des roches et physique des roches*

*en condition de grande profondeur*

*Felsmechanik und Felsphysik in grosser Tiefe*

*Editors / Rédacteurs / Redakteure*

V.MAURY & D.FOURMAINTRAUX

*Elf Aquitaine, Pau*

OFFPRINT / TIRE-A-PART



*Published for / Publié pour / Herausgegeben für*

*Le Comité Français de Mécanique des Roches*

A.A.BALKEMA / ROTTERDAM / BROOKFIELD / 1989